Dalton Transactions

PAPER

View Article Online
View Journal | View Issue

Cite this: *Dalton Trans.*, 2016, **45**, 13817

Synthesis of organic photosensitizers containing dithienogermole and thiadiazolo[3,4-*c*]pyridine units for dye-sensitized solar cells†

Yohei Adachi,[a] Yousuke Ooyama,[a] Naoyuki Shibayama[b] and Joji Ohshita*[a]

Received 20th June 2016,
Accepted 27th July 2016

DOI: 10.1039/c6dt02469f

www.rsc.org/dalton

Dithienogermole (DTG) is a germanium-bridged bithiophene system that has been applied as a building unit of conjugated materials for organic electronic devices, including organic photovoltaics and organic light emitting diodes. However, DTG has not been used as a component of sensitizers for dye-sensitized solar cells (DSSCs). In this work, we have synthesized three D–π-A–π-A type sensitizers containing DTG and thiadiazolo[3,4-*c*]pyridine (PTz). We expected that combining DTG and a strong acceptor PTz would give rise to a strong absorption in the visible region. In addition, we introduced bulky 2-ethylhexyl groups on the germanium atom to prevent dye aggregation on TiO_2 films. Three DTG-containing dyes with different anchor units were synthesized and their optical/electrochemical properties were investigated. The DTG-containing dyes exhibited broad and strong absorption bands around 600 nm on TiO_2. We fabricated DSSCs based on the DTG-containing dyes. The onsets of incident photon to current conversion efficiency (IPCE) spectra reached 900 nm and a maximal power conversion efficiency of 2.76% was achieved.

Introduction

Dye-sensitized solar cells (DSSCs) have been extensively studied as a photovoltaic system with potential applications in low-cost, flexible, and lightweight modules, since O'Regan and Grätzel reported high-performance DSSCs for the first time.[1] In this system, an organic dye adsorbed on a TiO_2 electrode absorbs sunlight to generate photocurrent. Thus, the design of the dye molecule is the key to improving cell performance. Currently, Ru-complex dyes, such as N3, N719, and black dye, are used to fabricate high-performance cells that exhibit over 10% power conversion efficiency (PCE).[2] Recently, Ru-free D (donor)–π-A (acceptor) type organic dyes have drawn attention as new low-cost photosensitizers. The D–A interaction in the π-conjugation system minimizes the HOMO–LUMO gap to extend dye absorption to the visible-NIR region, improving cell performance.[3]

Modified D–π-A systems have been examined to further improve the sensitizing properties of the dyes. For example, D–A–π-A and D–π-A–π-A type dyes that contain an additional acceptor linked by a π-spacer have been developed. It has been demonstrated that the introduction of a central acceptor unit, such as benzothiadiazole, quinoxaline, or diketopyrrolopyrrole, yields advantages such as photoenergy conversion in the NIR region, high electron injection efficiency, and improved stability of the sensitizers towards photoirradiation.[4] For example, as high as 9.04% and 8.50% PCEs were achieved in cells fabricated with benzothiadiazole- and quinoxaline-containing D–A–π-A dyes, respectively.[5] PCEs of 8.21% and 7.43% were achieved in cells made of benzothiadiazole (BT)- and diketopyrrolopyrrole-introduced D–π-A–π-A dyes.[6] Recently, thiadiazolo[3,4-*c*]pyridine (PTz, Chart 1) was used as the central acceptor of D–π-A–π-A dyes.[7] PTz is a stronger electron-withdrawing unit than common acceptors, such as BT and quinoxaline, because its extremely low-lying LUMO[8] gives rise to a strong absorption in the visible region.

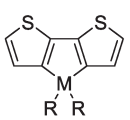

Dithienosilole (DTS, M=Si)
Dithienogermole (DTG, M=Ge)

Thiadiazolo[3,4-c]pyridine (PTz)

Chart 1 Structures of dithienosilole, dithienogermole, and thiadiazolo[3,4-*c*]pyridine.

[a]*Department of Applied Chemistry, Graduate School of Engineering, Hiroshima University, Higashi-Hiroshima 739-8527, Japan. E-mail: jo@hiroshima-u.ac.jp; Fax: +81-82-424-5494; Tel: +81-824-424-7743*

[b]*Technical Research Institute, Toppan Printing Co., Ltd, Takanodaiminami, Sugito, Saitama 345-8508, Japan*

†Electronic supplementary information (ESI) available: Experimental procedures, complemental electrochemical/optical spectra. See DOI: 10.1039/c6dt02469f

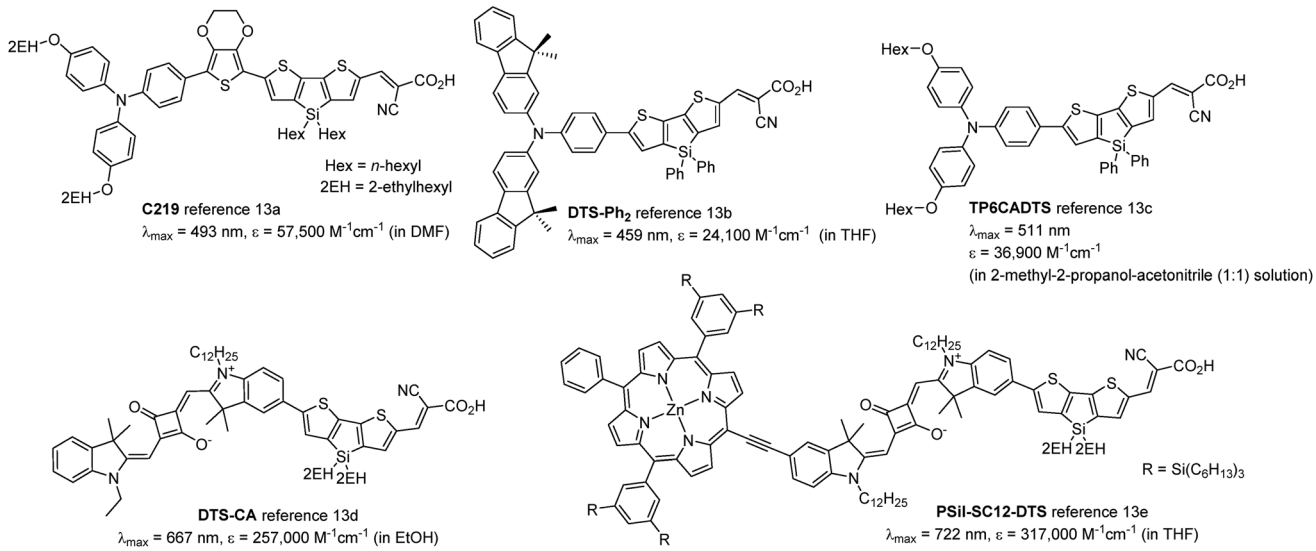

Chart 2 Structures of previously reported DTS-containing dyes.

Dithienosilole (DTS) and dithienogermole (DTG) are silicon- and germanium-bridged bithiophenes (Chart 1) that exhibit efficient conjugation because of their high planarity, and are useful as building units of π-conjugated optoelectronic materials. DTS and DTG show interesting interactions between the Si–C or Ge–C σ*-orbitals and the π*-orbital of the bithiophene unit (σ*–π* interaction), which lowers LUMO energy levels and further reduces the HOMO–LUMO gaps of the compounds.[9] DTS- and DTG-containing π-conjugated oligomers and polymers have been applied to organic photovoltaics[10,11] and organic light emitting diodes.[10,12] Ko *et al.* reported that photosensitizers with DTS as the π-conjugated linker exhibited electron injection readily from the photoexcited dyes to TiO_2, due to the low-lying LUMO energy level (Chart 2).[13b] In addition, bulky substituents on the DTS silicon atom hindered not only contact between the electrolyte and the TiO_2 surface, but also dye aggregation on TiO_2. This furnished cells with high short-circuit current density (J_{sc}) and open circuit voltage (V_{oc}). Jradi *et al.* reported that the introduction of 2-ethylhexyl-substituted DTS as the π-linker effectively suppressed dye aggregation on the TiO_2 surface, which resulted in the high V_{oc} and J_{sc} of the DSSCs.[13d,e] Zeng *et al.* also reported 7.6% PCE in a DSSC based on a DTS-containing dye with a simple D–π-A structure under standard global AM 1.5G solar irradiation of one sun (Chart 2).[13a]

In this report, we introduced PTz as the central acceptor unit of the D–π-A–π-A system to narrow the HOMO–LUMO gaps of the dyes. We also used DTG as the π-spacer unit for the first time. Previously, Welch, Bazan *et al.* synthesized molecular dyes with PTz as electron-acceptors and DTG or DTS as an electron-donor.[14] These dyes had strong absorption in the visible region with the edges reaching 800 nm in solution, regardless of the bridging elements, *i.e.* Si or Ge. We therefore expected that the introduction of DTG in place of DTS may also yield an effective conjugation in the present dyes. As DTG has longer Ge–C (substituent) bonds than DTS, it is speculated that the longer bond would affect the dye aggregation on TiO_2 by expanding inter-dye distances. It was also expected that the low polarization of Ge–C bonds compared with that of Si–C bonds would stabilize the π-systems towards hydrolysis, making hydrolytic synthetic transformation possible. This, for example, enabled the synthesis of a DTG-containing carboxylic acid derivative by alkali-catalyzed hydrolysis of the corresponding ester, in contrast to the analogous DTS compound whose silole ring underwent decomposition under the same conditions. Furthermore, DTG would be more stable than DTS towards oxidation, as Ge–O bonds (659.4 kJ mol^{-1}) are usually weaker than Si–O bonds (799.6 kJ mol^{-1}), while Ge–C and Si–C bonds have similar bond energies (460 kJ mol^{-1} and 451.5 kJ mol^{-1}).[15]

Results and discussion

Synthesis

The procedures for the synthesis of the donor and acceptor units are shown in Schemes 1 and 2, respectively, using Stille and Suzuki cross coupling as the key reactions. **DTGBr**[11f] and **PTzBr2**[16] were synthesized according to the literature. Bulky 2-ethylhexyl groups were introduced on the Ge atom to enhance solubility and prevent aggregation upon adsorption to TiO_2. As the Lewis basicity of PTz is too weak to allow coordination to the TiO_2 surface, three anchor groups (pyridyl, carboxylic, and cyanoacrylic groups) were introduced. They were also expected to serve as additional acceptors. The D–π-A–π-A dye **DTGPTzPy** was synthesized by Stille cross coupling of **DTGSn** and **PTzTPy** (Scheme 3).

In general, to synthesize simple carboxylic acid derivatives, corresponding esters are hydrolyzed under strong alkali conditions. Thus, we carried out control experiments to evaluate

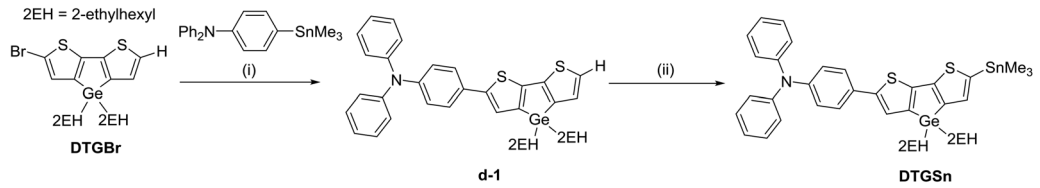

Scheme 1 Reagents and conditions: (i) toluene, $Pd_2(dba)_3$, P(*o*-tol)$_3$, 100 °C, 1.5 d; (ii) (1) CH_2Cl_2, NBS, (2) THF, *n*BuLi, Me_3SnCl, −78 °C, overnight.

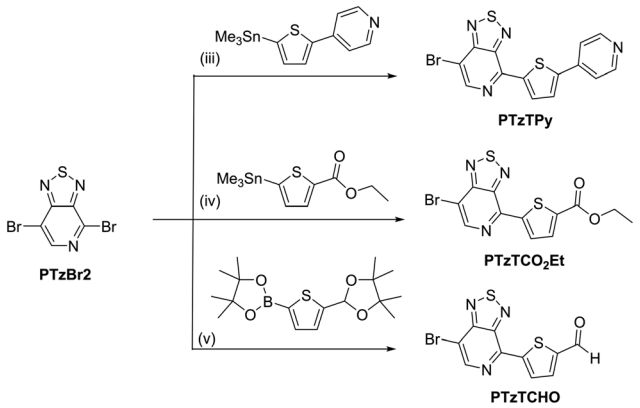

Scheme 2 Reagents and conditions: (iii) DMF, $Pd(PPh_3)_4$, 120 °C, 1 h; (iv) toluene, $Pd_2(dba)_3$, P(*o*-tol)$_3$, 60 °C, 5 h; (v) (1) THF/H_2O, $Pd(PPh_3)_4$, Na_2CO_3, 70 °C, overnight, (2) THF/H_2O, HCl, reflux, overnight.

the stability of DTG under alkali conditions. Treatment of **DTG(2EH)** with aq. NaOH caused no reaction, whereas treatment of **DTS(2EH)** provided a Si–C hydrolyzed product (Fig. 1 and S1†). This indicates the higher stability of DTG towards hydrolysis. As expected, the hydrolysis of **DTGPTzCO2Et** by aq. NaOH provided **DTGPTzCA**, although the yield was low (16%). This low yield may be attributed to the stronger reaction conditions than those of the control experiment. Under the same strong alkali conditions, the corresponding DTS derivative would not be prepared, as DTS is less stable than DTG. Cyanoacrylic acid derivative **DTGPTzCA2** was synthesized by the Knoevenagel condensation in good yield (Scheme 3). All the new compounds were identified by ^{1}H NMR, ^{13}C NMR, and HR-MS analysis.

Photophysical properties

Fig. 2 shows the UV-vis absorption spectra of the dyes in THF. All the dyes exhibited two absorption bands around 410 nm and 600 nm. For the bands around 600 nm, that of **DTGPTzCA2** appeared at the lowest energy of the three DTG-containing dyes, likely because of the strong electron-withdrawing properties of the cyanoacrylic group. The molar extinction coefficients were similar to those of the previously reported PTz-containing D–π-A–π-A dyes.[7] When compared to previously reported DTS-based dyes, the present DTG-dyes had comparable[13a–c] or small[13d,e] molar extinction coefficients, presumably due to the difference in other π-systems in the molecules. Those bands are red-shifted by approximately 100 nm compared to the previously reported D–π-A type DTS analogues (Chart 2),[13a–c] which is obviously attributed to the strong electron-accepting properties of PTz. In THF containing 1 vol% trifluoroacetic acid (TFA), the absorption bands around 600 nm of **DTGPTzPy** and **DTGPTzCA2** were red-shifted by 20 nm and 14 nm, respectively (Table 1). The shifts were likely due to the protonation of the anchor units. On the other hand, the spectrum of **DTGPTzCA** was unchanged by the TFA addition. These results indicated that the carboxylic group of **DTGPTzCA** was not deprotonated in neutral THF, whereas the cyanoacrylic group of **DTGPTzCA2** formed a separated ion pair even in neutral THF, which was converted into neutral acid in TFA/

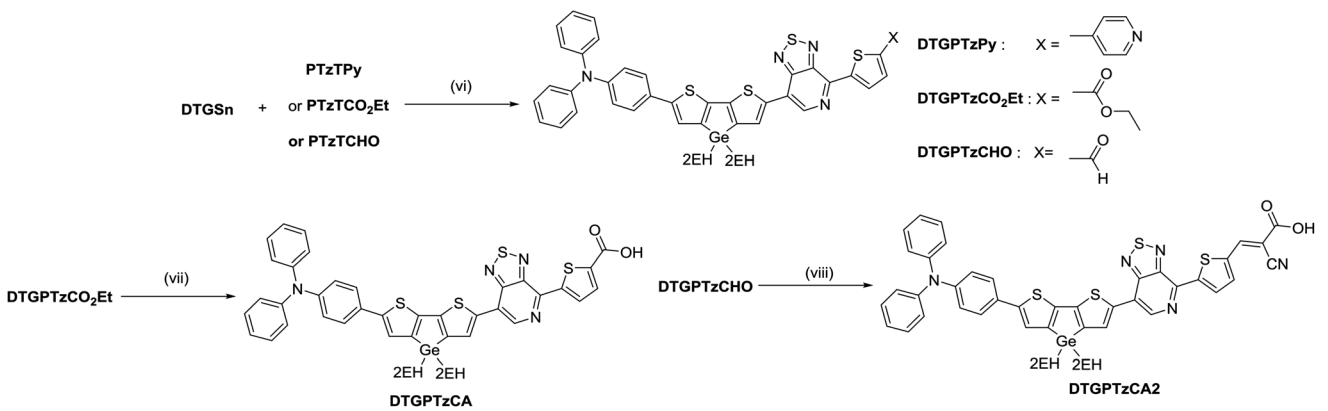

Scheme 3 Reagents and conditions: (vi) toluene, $Pd_2(dba)_3$, P(*o*-tol)$_3$, 60 °C, 4 h; (vii) THF/H_2O, NaOH, reflux, 5 h; (viii) MeCN/$CHCl_3$, cyanoacetic acid, piperidine, reflux, overnight.

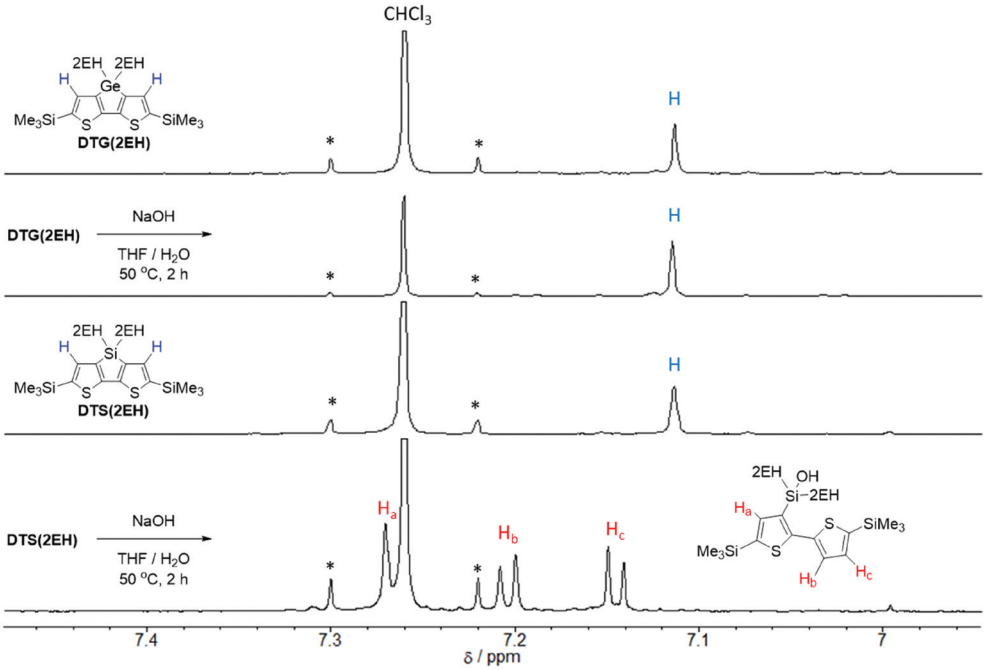

Fig. 1 ^{1}H NMR spectra of **DTG(2EH)** and **DTS(2EH)** before and after the control experiment (aromatic region).

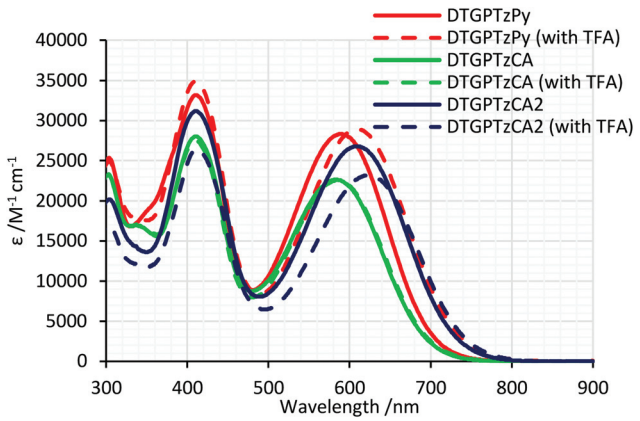

Fig. 2 UV-vis absorption spectra of DTG-containing dyes in THF with or without TFA.

THF. The absorption band shift of **DTGPTzPy** was ascribed to the formation of a pyridinium salt. As a consequence, it was found that the absorption bands of the neutral dyes shifted to the longer wavelength region in the following order: **DTGPTzCA** < **DTGPTzPy** < **DTGPTzCA2**.

The normalized and non-normalized absorption spectra of DTG-containing dyes attached to the TiO_2 thin film are shown in Fig. 3 and S2,† respectively. The spectrum of **DTGPTzPy** showed a slight red shift of the absorption band around 600 nm relative to that in solution. In contrast, the spectrum of **DTGPTzCA** exhibited a slight blue shift. For **DTGPTzPy**, the pyridyl moiety would interact with the Lewis acidic site on the TiO_2 surface to become more cationic than that in solution, which would enhance the electron-withdrawing properties of the pyridyl moiety and narrow the HOMO–LUMO gap. On the other hand, the carboxylic group would become more anionic by forming CO_2–Ti bonds on the TiO_2 surface, which would lead to the blue-shifted spectrum of **DTGPTzCA**. We expected a similar blue shift in the case of **DTGPTzCA2**. However, we

Table 1 Photophysical and electrochemical properties of DTG-containing dyes

Dye	λ_{max}/nm	ε^{c}/M^{-1} cm^{-1}	λ_{max} (on TiO_2)^{d}/nm	HOMO/eV	$E_g{}^{g}$/eV	LUMO^{h}/eV
DTGPTzPy	589, 411^{a}	28 300, 33 200	601, 426	−5.03^{e}	1.77	−3.26
DTGPTzPy (TFA added)	609, 410^{b}	28 900, 34 900	—	−5.05^{f}	1.69	−3.36
DTGPTzCA	583, 410^{a}	22 800, 28 100	577, 419	−5.04^{e}	1.78	−3.26
DTGPTzCA2	609, 411^{a}	26 800, 31 300	649, 453	−5.00^{e}	1.71	−3.29
DTGPTzCA2 (TFA added)	623, 412^{b}	23 300, 26 400	—	−5.05^{f}	1.67	−3.38

^{a} Absorption maxima in neutral THF. ^{b} In THF containing 1 vol% TFA (0.0120 mM). ^{c} Molar extinction coefficient. ^{d} Absorption maxima on the TiO_2 film without CDCA. ^{e} HOMO was determined from the oxidative potential in CV measurements in neutral DMF. ^{f} In DMF containing 1 vol% TFA (0.5 mM). ^{g} E_g (HOMO–LUMO gap) was determined from the onset of absorption spectra. ^{h} LUMO was calculated from HOMO + E_g.

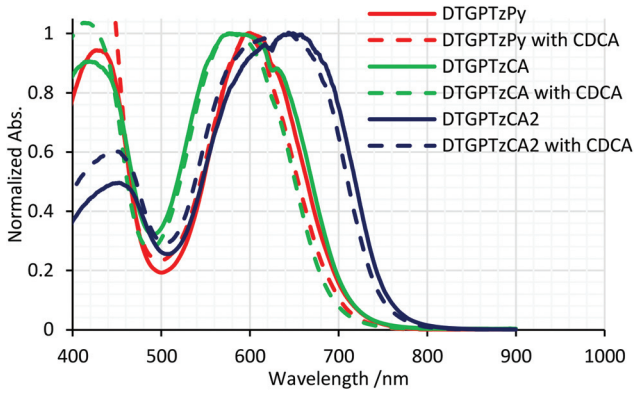

Fig. 3 Normalized UV-vis absorption spectra of DTG-containing dyes on TiO_2 films; **DTGPTzPy**, **DTGPTzCA**, and **DTGPTzCA2** were also co-adsorbed with 0.5 mM, 1.0 mM, and 2.0 mM CDCA, respectively.

obtained a broadened and red-shifted absorption compared with that in solution. This tendency may be attributed to dye aggregation. We speculated that the dipole moment of **DTGPTzCA2** should be larger than that of **DTGPTzCA**, because of the electron-withdrawing properties of the cyano group. In general, a large dipole moment enhances intermolecular interaction. In addition, the amount of dye loading of **DTGPTzCA2** was larger than that of **DTGPTzCA** (Table 2, *vide infra*). We also speculated that the large amount of dye-loading induced the dye aggregation. However, we could not find solid evidence of the dye aggregation. When co-adsorbed with chenodeoxycholic acid (CDCA), the absorbance was decreased and dye loading was minimized (Fig. S2† and Table 2). However, the shape of the spectra was unchanged (Fig. 3). Hence, we speculated that inter-dye interactions on the TiO_2 surface were not strong. This seemed to be caused by the long Ge–C (substituent) bonds, which sterically separated the dye molecules.

Electrochemical properties

To evaluate electron injection ability and regeneration of the present dyes, cyclic voltammogram (CV) measurements were performed in DMF containing tetrabutylammonium perchlorate (0.1 M) under nitrogen (Fig. S3†). For **DTGPTzPy** and **DTGPTzCA2**, measurements under acidic conditions with 1 vol% TFA were also carried out. The CVs have pseudo-reversible properties. It may be considered that the DTG-based dyes are not stable in the DSSC system. The irreversible properties, however, were likely due to the addition of nucleophiles, such as a perchlorate anion, to oxidized molecules. Thereafter, in the absence of nucleophiles, the DTG units would be stable, and in fact, heating **DTG(2EH)** in a DSSC redox solution, *i.e.* in CD_3CN containing 0.05 M I_2/0.1 M LiI, at 75 °C, for 2 days caused no decomposition of the compound, indicating the stability of DTG units under these conditions. The HOMO energy levels of the dyes were estimated from the anodic onsets (E_{ox}, HOMO = −4.8 − E_{ox}) (Table 1). They were more negative than the iodide/triiodide redox potential (−4.8 eV), indicating that the dye regeneration in DSSC may readily proceed by electron transfer from the redox solution. The HOMO–LUMO energy gaps (E_g) were obtained from the onset of absorption spectra in solution. The LUMO energy levels were estimated by HOMO + E_g. The small E_g of the dyes in the range of 1.60–1.80 eV seemed to reflect the effective conjugation in the D–π-A–π-A system. The LUMO energy levels were more positive than the conduction band edge of TiO_2 (−3.9 eV), which was desirable for photoelectron injection. The HOMO–LUMO gaps of **DTGPTzPy** and **DTGPTzCA** were nearly the same, whereas that of **DTGPTzCA2** was slightly smaller. This difference may be due to the stronger electron-withdrawing properties of the cyanoacrylic group than those of the pyridyl group and the simple carboxylic group.

Under acidic conditions, E_{ox} of **DTGPTzPy** and **DTGPTzCA2** was slightly shifted to the positive potentials. This meant that the HOMO energy levels were lowered by the protonation of the anchors.

Theoretical calculations

To elucidate the geometrical and electronic properties, density functional theory (DFT) calculations of the three dye models that bear methyl groups in place of 2-ethylhexyls on the Ge atom were carried out by using the Gaussian 09 program at the B3LYP/6-31G(d) level of theory. The optimized geometries in the gas phase and the frontier orbital profiles are shown in Fig. 4. The HOMOs were delocalized mainly on the donor units of triphenylamine and the π-spacer of DTG, and the LUMOs were distributed over the PTz, thiophene π-spacer, and anchor acceptor units. These separated HOMO and LUMO distributions would contribute to effective intramolecular charge-transfer (ICT), consistent with the strong absorption bands around 600 nm of the real compounds. Despite that, the phenylene and DTG moieties were twisted by approximately 23° with respect to the interplane angles, and the delocalized HOMOs indicated efficient conjugation between the triphenylamine and DTG units. For **DTGPTzCA** and **DTGPTzCA2**, the

Table 2 Photovoltaic properties of DSSCs based on the three dyes in full sunlight (AM 1.5G, 100 mW cm^{-2})

Dye		J_{sc}/mA cm^{-2}	V_{oc}/V	FF	PCE/%	Dye loading/10^{16} mol cm^{-2}
DTGPTzPy	Without CDCA	5.16	0.41	0.62	1.31	3.39
	With 0.5 mM CDCA	9.52	0.43	0.67	2.76	1.65
DTGPTzCA	Without CDCA	4.93	0.46	0.64	1.45	7.65
	With 1.0 mM CDCA	7.12	0.48	0.66	2.29	4.48
DTGPTzCA2	Without CDCA	4.23	0.35	0.59	0.88	8.12
	With 2.0 mM CDCA	6.11	0.37	0.60	1.36	6.41

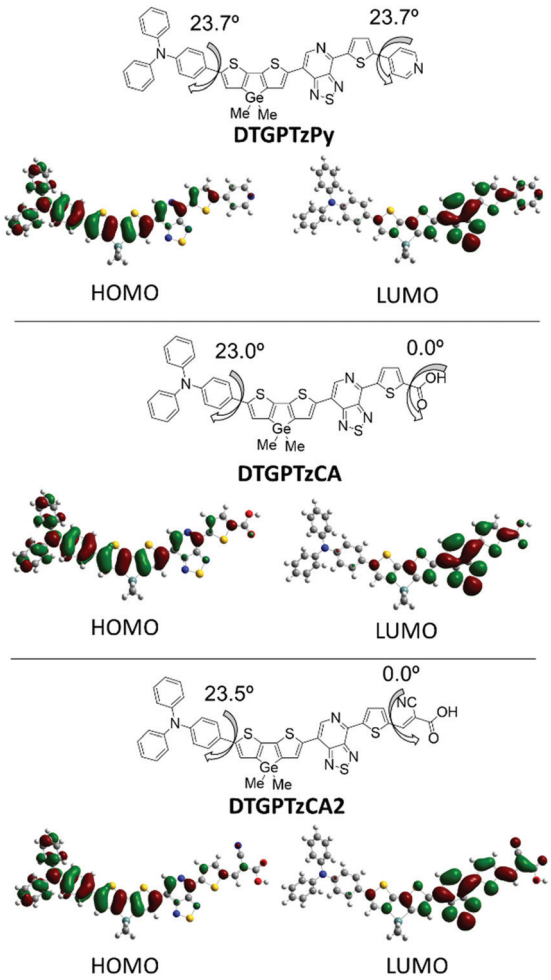

Fig. 4 Frontier orbitals of DTG-containing dyes calculated by the DFT at B3LYP/6-31G(d) level.

high planarity of the A–π-A fragment, including the PTz ring and adjacent π-conjugated units, also led to enhanced conjugation. In the case of **DTGPTzPy**, the torsional angle between the thiophene π-spacer and the pyridyl moiety was computed to be 23.7°. This twisting may bring about a decline of the photoelectron injection efficiency, because the LUMO orbital is not sufficiently spread to the pyridyl anchor moiety.

Photovoltaic properties

We fabricated DSSCs based on the present three DTG-containing dyes as sensitizers. The electrolyte was composed of 0.6 M 1,2-dimethyl-3-propylimidazolium/0.05 M I_2/0.1 M LiI and the cell effective area was 0.25 cm^2. TiO_2 electrodes were modified with 0.1 mM dye solution for 15 hours. Co-adsorption with CDCA was also examined to prevent aggregation of the dyes on TiO_2.

The IPCE spectra of the fabricated cells are shown in Fig. 5. (IPCE = LHE × φ_{inj} × φ_{reg} × η_{cc}, where LHE is light-harvesting efficiency, LHE = 1–10^{-A}, A is the absorbance of the film, φ_{inj} and φ_{reg} are electron injection and dye regeneration efficiencies, respectively, and η_{cc} is the charge collection efficiency.[17])

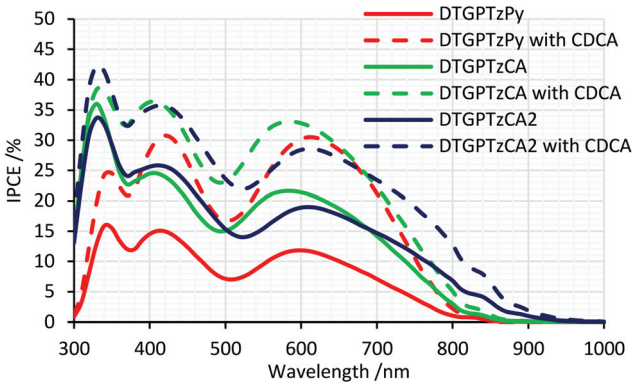

Fig. 5 IPCE spectra of DSSCs based on DTG-containing dyes.

As shown in Fig. 5, the IPCE values were not very high. LHEs were estimated to be higher than 90% in the range of 400–700 nm from the absorbance of the dye-adsorbed TiO_2 film (Fig. S2†). Therefore, the relatively low IPCE would be attributed to some other factors. For example, the evaluated HOMO and LUMO energy levels of the dyes in solution would not be always consistent with those on the TiO_2 surface because the dyes interact with TiO_2 strongly; thus, the HOMO energy levels of the dyes might be too close to the potential of the iodide/triiodide redox couples on TiO_2, which would reduce dye regeneration efficiency. The onsets of the IPCE spectra reached NIR wavelengths. Particularly, DSSC based on **DTGPTzCA2** showed photoelectronic conversion up to 900 nm. The *J*–*V* curves of the fabricated DSSCs without CDCA are shown in Fig. 6. Although the amount of dye loading of **DTGPTzPy** was less than half of that of **DTGPTzCA**, the J_{sc} values were nearly the same (Table 2). This result is consistent with the previous report that DSSCs with dyes containing a pyridyl anchor showed superior performance to analogous dyes with a carboxylic anchor, in terms of electron injection efficiency.[18] Next, we optimized the cells by co-adsorption with CDCA (Fig. 7). Cell performance was improved and maximized with 0.5 mM CDCA for **DTGPTzPy**, 1.0 mM CDCA for **DTGPTzCA**, and 2.0 mM CDCA for **DTGPTzCA2**. In particular, the perform-

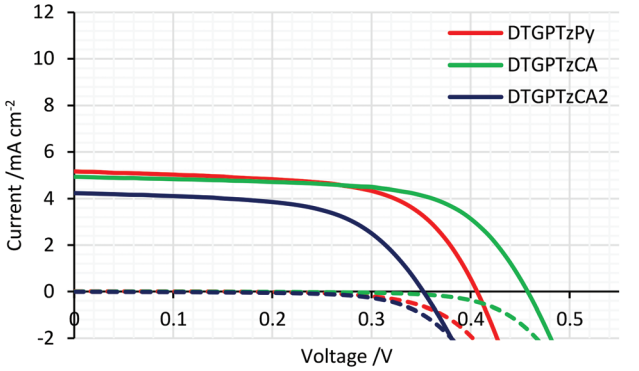

Fig. 6 *J*–*V* curves of DSSCs based on DTG-containing dyes without CDCA. Dark current/potential relationships are shown by dashed lines.

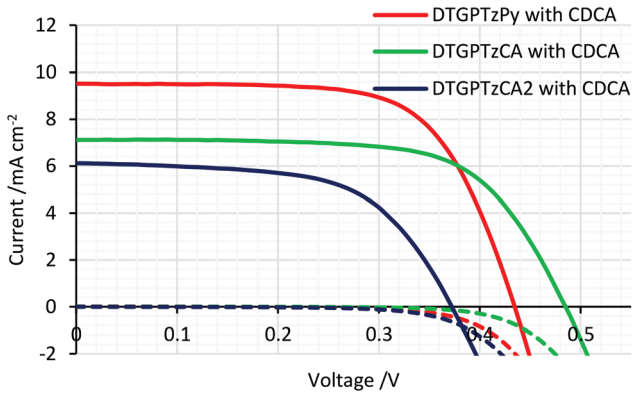

Fig. 7 *J*–*V* curves of DSSCs based on DTG-containing dyes with CDCA. Dark current/potential relationships are shown by dashed lines.

ance of the device with **DTGPTzPy** was dramatically improved with high J_{sc} of 9.52 mA cm^{-2} to reach a PCE of 2.76%.

Electrochemical impedance spectroscopy

We carried out electrochemical impedance spectroscopy (EIS) measurements to evaluate the interfacial charge recombination process in the DSSCs. The measurements were performed under a forward bias of V_{oc} in the dark. The Bode plots and the Nyquist plots are shown in Fig. 8 and S4,† respectively, and the electron lifetimes (τ_e) and the electron transport resistances (R_{rec}) are summarized in Table 3. A long electron lifetime leads to a high charge collection efficiency and the larger

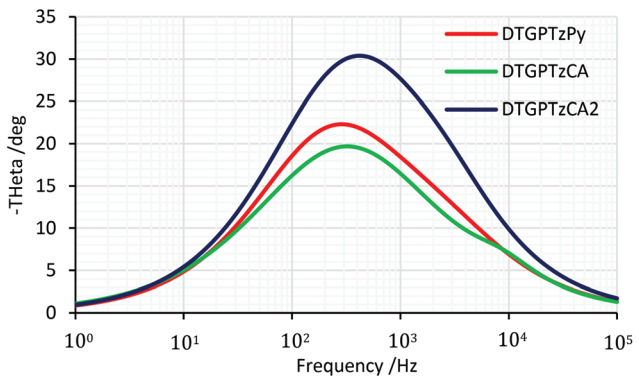

Fig. 8 EIS Bode plots of DSSCs based on DTG-containing dyes.

Table 3 Electron lifetimes and electron transport resistances of DSSCs based on DTG-containing dyes

Dye	τ_e [a]/ms	R_{rec} [b]/ohm cm^{-1}
DTGPTzPy	0.50	63.8
DTGPTzTCA	0.50	59.2
DTGPTzTCA2	0.40	102.5

[a] Electron lifetime in the TiO_2 film. [b] Electron transport resistance among the TiO_2/dye/electrolyte.

semicircle in the Nyquist plots indicates higher charge transport resistance and thus improved V_{oc}. The electron lifetimes of the DSSCs based on the three dyes were estimated to be 0.4–0.5 ms, which were much shorter than that of the previously reported DTS-containing dye.[13c] This short lifetime indicates a fast back electron transfer from TiO_2 to the dye, lowering V_{oc}.

Conclusions

In summary, we synthesized new D–π-A–π-A type organic sensitizers with DTG and PTz as a π-conjugated spacer and a strong acceptor, respectively. **DTGPTzCA** was synthesized *via* the hydrolysis of the ester group, which proved that the DTG unit was stable to reactions under strong basic conditions. The synthesized DTG-containing dyes showed strong absorption in the visible and NIR regions, of which the absorption onset of **DTGPTzCA2** on TiO_2 reached 900 nm. The effective D–A interaction was supported by DFT calculations. The synthesized dyes were applicable to DSSCs and the best PCE of 2.76% was obtained for the DSSC based on **DTGPTzPy** co-adsorbed with CDCA. Although the PCEs of DSSCs based on DTG-containing dyes were not very high, the photoelectric conversion ranges were excellent as compared to previously reported DSSCs based on PTz-containing D–π-A–π-A type dyes[7] and DTS-based dyes,[13] which have the IPCE onsets from 700 to 850 nm.

Experimental

General

NMR spectra were recorded on Varian System 500 and Varian 400MR spectrometers. HR-MS spectral data were acquired on a Thermo Fisher Scientific LTQ Orbitrap XL spectrometer. Melting points were measured with a Yanaco MP-500P system in air. UV-Vis absorption spectra in solution were obtained with a Hitachi U-2910 spectrometer and those on TiO_2 films were recorded with a Shimadzu UV-3150 with an ISR-3100 integrating sphere by the reflection method and converted into absorption using the Kubelka–Munk formula. Cyclic voltammograms were measured with an AMETEK VersaSTAT 4 potentiostat/galvanostat in a solution of 0.1 M tetrabutylammonium perchlorate (TBAP) in DMF using a three-electrode system with a Pt plate counter electrode, a Pt wire working electrode, and an Ag/Ag$^+$ reference electrode.

All reactions were carried out under dry argon. As the reaction solvents, THF, toluene, and MeCN were purchased from Kanto Chemical Co., Ltd. They were distilled from calcium hydride and stored over activated molecular sieves until use. Chloroform was purchased from Kanto Chemical Co., Ltd and distilled from calcium hydride immediately before use. Usual workup mentioned below included hydrolysis of the reaction mixture with water and separation of the organic layer. The aqueous layer was extracted with toluene, chloroform, and ethyl acetate. The organic layer and the extract were combined

and washed with water. After drying over anhydrous magnesium sulfate, the solvent was evaporated.

Synthesis of DTGPTzPy. A mixture of 118 mg (0.136 mmol) of **DTGSn**, 50.2 mg (0.134 mmol) of **PTzTPy**, 7.0 mg (5 mol%) of $Pd_2(dba)_3$, 8.7 mg (20 mol%) of P(*o*-tol)$_3$, and 5 mL of toluene was heated at 60 °C for 4 h with stirring. After usual workup using chloroform for extraction, the residue was purified by preparative GPC with toluene as an eluent to give a diastereomeric mixture of 60.8 mg (60.7 μmol, 45% yield) of **DTGPTzPy**: dark greenish powder, m.p.: 73–76 °C. ^{1}H NMR (in CD_2Cl_2): δ = 0.80–0.92 (12H, m, CH_3), 1.18–1.44 (20H, m, CH_2), 1.57–1.67 (2H, m, CH), 7.01–7.09 (4H, m, *p*-Ph and phenylene), 7.12 (4H, dd, J = 8.8, 1.2 Hz, *o*-Ph), 7.26 (1H, s, DTG), 7.27–7.32 (4H, m, *m*-Ph), 7.45 (2H, d, J = 8.4 Hz, phenylene), 7.51–7.56 (2H, m, pyridyl), 7.54 (1H, d, J = 4.0 Hz, thiophene), 8.16 (1H, m, DTG), 8.51 (1H, d, J = 4.0 Hz, thiophene), 8.55–8.59 (2H, m, pyridyl), 8.70 (1H, m, PTz). ^{13}C NMR (in CD_2Cl_2): δ = 11.1, 11.2, 14.4, 21.3, 23.50, 23.52, 29.25, 29.28, 29.5, 36.0, 37.55, 37.57, 120.1, 122.0, 123.6, 124.0, 125.0, 125.7, 126.8, 127.3, 128.9, 129.8, 131.9, 132.5, 137.3, 139.9, 141.1, 143.9, 144.5, 144.88, 144.90, 145.0, 145.66, 145.68, 145.72, 146.58, 146.60, 146.62, 147.63, 147.67, 147.70, 147.9, 148.4, 149.7, 150.9, 154.8. HR-MS (APCI) Calcd for $C_{56}H_{57}GeN_5S_4$: M^+: 1001.27031, Found: 1001.27148.

Synthesis of DTGPTzCO2Et. Ester **DTGPTzCO2Et** was obtained in a fashion similar to that of **DTGPTzPy** from **DTGSn** and **PTzTCO2Et** in 77% yield as a diastereomeric mixture: dark greenish powder, m.p.: 39–40 °C. ^{1}H NMR (in CD_2Cl_2): δ = 0.78–0.85 (12H, m, CH_3 in 2EH), 1.16–1.43 (23H, m, CH_2 in 2EH and CH_3 in EtO), 1.50–1.60 (2H, m, CH in 2EH), 4.38 (2H, q, J = 6.8 Hz, CH_2 in EtO), 7.04–7.09 (4H, m, *p*-Ph and phenylene), 7.12 (4H, dd, *o*-Ph, J = 8.8, 1.2 Hz), 7.26–7.33 (5H, m, DTG and *m*-Ph), 7.51 (2H, d, J = 8.8 Hz, phenylene), 7.88 (1H, d, J = 4.0 Hz, thiophene), 8.25 (1H, m, DTG), 8.61 (1H, d, J = 4.0 Hz, thiophene), 8.87 (1H, m, PTz). ^{13}C NMR (in CD_2Cl_2): δ = 11.17, 11.22, 14.42, 14.43, 14.6, 21.22, 21.25, 21.29, 23.51, 23.53, 29.25, 29.29, 29.5, 36.0, 37.55, 37.57, 61.8, 122.6, 123.6, 123.9, 125.0, 125.71, 126.74, 128.9, 129.8, 131.0, 132.3, 134.4, 136.9, 137.2, 139.7, 144.0, 144.8, 145.70, 145.72, 145.8, 146.71, 146.73, 146.8, 147.6, 147.78, 147.85, 147.89, 147.93, 148.0, 148.4, 150.0, 154.7, 162.5. HR-MS (APCI) Calcd for $C_{54}H_{58}GeN_4O_2S_4$: $[M + H]^+$: 997.27271, Found: 997.27105.

Synthesis of DTGPTzCHO. Aldehyde **DTGPTzCHO** was obtained in a fashion similar to that of **DTGPTzPy** from **DTGSn** and **PTzTCHO** in 91% yield as a diastereomeric mixture: dark greenish powder, m.p.: 67–69 °C. ^{1}H NMR (in CD_2Cl_2): δ = 0.80–0.91 (12H, m, CH_3), 1.19–1.48 (20H, m, CH_2), 1.59–1.69 (2H, m, CH), 7.02 (2H, d, J = 8.8 Hz, phenylene), 7.04–7.09 (2H, m, *p*-Ph), 7.12 (4H, dd, J = 8.8, 1.2 Hz, *o*-Ph), 7.25 (1H, s, DTG), 7.26–7.32 (4H, m, *m*-Ph), 7.42 (2H, d, J = 8.8 Hz, phenylene), 7.75 (1H, d, J = 4.0 Hz, thiophene), 8.21 (1H, m, DTG), 8.53 (1H, d, J = 4.0 Hz, thiophene), 8.70 (1H, m, PTz), 9.90 (1H, s, CHO). ^{13}C NMR (in CD_2Cl_2): δ = 11.1, 11.2, 14.41, 14.42, 21.10, 21.13, 21.2, 23.48, 23.50, 29.18, 29.22, 29.4, 36.0, 37.47, 37.49, 123.0, 123.6, 123.8, 125.0, 125.6, 126.7, 128.7, 129.7, 131.2, 132.43, 132.45, 132.48, 137.00, 137.01, 137.4, 139.5, 143.3, 144.65, 144.67, 144.69, 145.5, 145.72, 145.74, 145.8, 146.85, 146.88, 146.90, 147.6, 147.8, 148.0, 148.0, 148.1, 148.4, 150.46, 150.49, 154.4, 183.6. HR-MS (APCI) Calcd for $C_{52}H_{54}GeN_4OS_4$: $[M + H]^+$: 953.24650, Found: 953.24707.

Synthesis of DTGPTzCA. In a mixture of 20 mL of THF, 3 mL of 1 M aq. NaOH, and 12 mL of water was dissolved 95.2 mg (95.6 μmol) of **DTGPTzCO2Et**. After the solution was heated to reflux for 5 h with stirring, the reaction mixture was neutralized by adding 10% aq. HCl. After usual workup using ethyl acetate for extraction, the residue was subjected to silica gel column chromatography using a mixture of hexane/acetic acid = 99/1 as an eluent to give a diastereomeric mixture of 16.0 mg (16.5 μmol, 17% yield) of **DTGPTzCA**: dark greenish solid, m.p.: 81–84 °C. ^{1}H NMR (in CD_2Cl_2): δ = 0.75–1.66 (34H, m), 6.99 (2H, br d, J = 8.4 Hz), 7.02–7.13 (6H, m, *o*-Ph and *p*-Ph), 7.22 (1H, s, DTG), 7.23–7.30 (4H, m, *m*-Ph), 7.40 (2H, br d, J = 8.4 Hz, phenylene), 7.85 (1H, br s, thiophene), 8.13 (1H, br s, DTG), 8.42 (1H, br s, thiophene), 8.72 (1H, br s, PTz). ^{13}C NMR (in CD_2Cl_2): δ = 11.15, 11.20, 14.41, 14.42, 21.2, 21.3, 23.51, 23.53, 29.25, 29.29, 29.5, 36.1, 37.5, 37.6, 122.8, 123.6, 123.9, 125.0, 125.7, 126.8, 129.0, 129.8, 131.1, 132.1, 136.0, 137.1, 139.6, 143.8, 144.9, 145.7, 146.8, 147.6, 147.9, 148.4, 149.3, 150.4, 154.6. HR-MS (APCI) Calcd for $C_{52}H_{54}GeN_4O_2S_4$: $[M + H]^+$: 969.24141, Found: 969.24146.

Synthesis of DTGPTzCA2. A mixture of 112 mg (0.118 mmol) of **DTGPTzCHO**, 22.8 mg (0.268 mmol) of cyanoacetic acid, 6 μL of piperidine, and 20 mL of a mixed solvent of acetonitrile/chloroform = 1/1 was heated to reflux overnight. The solvent was evaporated and the residue was subjected to silica gel chromatography with ethyl acetate to elute unreacted ester and byproducts. Then, **DTGPTzCA2** was eluted with methanol to give a diastereomeric mixture of 104 mg (0.102 mmol, 86%) of **DTGPTzCA2**: dark greenish powder, m.p.: 145–146 °C. ^{1}H NMR (in DMSO-d_6): δ = 0.70–0.82 (12H, m, CH_3), 1.00–1.44 (20H, m, CH_2), 1.44–1.57 (2H, m, CH), 6.96 (2H, d, J = 8.4 Hz, phenylene), 7.03–7.12 (6H, m, Ph), 7.33 (4H, t, J = 8.0 Hz, *m*-Ph), 7.48 (1H, br s, DTG), 7.54 (2H, d, J = 8.4 Hz, phenylene), 7.81 (1H, d, J = 4.0 Hz, thiophene), 8.14 (1H, s, olefin), 8.31 (1H, br s, DTG), 8.55 (1H, d, J = 4.0 Hz, thiophene), 8.94–8.99 (1H, m, PTz). ^{13}C NMR spectrum was not obtained because of the low solubility of the product. HR-MS (ESI) Calcd for $C_{55}H_{55}GeN_5O_2S_4$: M^+: 1019.24449, Found: 1019.24554.

Cell fabrication and characterization

A layer of TiO_2 paste (PST-18NR, JGC Catalysts and Chemicals Ltd, Japan) was formed on an FTO substrate by the doctor blade technique. The electrodes were sintered for 45 min at 450 °C to coat the surface with an approximately 9 μm thick TiO_2 film, which was shaved to 0.5 × 0.5 cm^2 as the photoactive area. The sintered electrodes were immersed in 0.1 mM dye solution in THF for 15 h. Dye loading was estimated by subtracting the concentration of the dye solution after immersion from that before immersion, on the basis of UV-vis absorbance measurements. The cells were fabricated with the modified TiO_2 electrode with Pt-vapored glass as the counter electrode, a spacer, and an electrolyte composed of 0.05 M iodine, 0.1 M

lithium iodide, and 0.6 M 1,2-dimethyl-3-propylimidazolium iodide in acetonitrile.

The photocurrent–voltage (*I–V*) characteristics of the DSSCs were measured on a Keithley 2611A source meter under AM 1.5, 100 mW cm^{-2} (1 sun) irradiation by a solar simulator (Bunkoukeiki Co., Ltd, OTENTO-SUN III). The incident light intensity was calibrated with a reference Si solar cell equipped with a heat absorbing filter (Bunkoukeiki Co., Ltd, BS520BK). The IPCE spectra were recorded with an SM-250 (Bunkoukeiki Co., Ltd). The active areas of the TiO_2 films were determined with a KEYENCE VHX-1000 digital microscope.

EIS measurements were performed on the same DSSCs in the dark under a forward bias of V_{oc} using an AMETEK Versa-STAT 3 potentiostat/galvanostat.

Acknowledgements

This work was supported by a Grant-in-Aid for Scientific Research (B) (JSPS KAKENHI Grant No. 26288094).

Notes and references

1 B. O'Regan and M. Grätzel, *Nature*, 1991, **353**, 737–740.
2 (*a*) M. K. Nazeeruddin, P. Péchy, T. Renouard, S. M. Zakeeruddin, R. Humphry-Baker, P. Comte, P. Liska, L. Cevey, E. Costa, V. Shklover, L. Spiccia, G. B. Deacon, C. A. Bignozzi and M. Grätzel, *J. Am. Chem. Soc.*, 2001, **123**, 1613–1624; (*b*) M. Grätzel, *J. Photochem. Photobiol., A*, 2004, **164**, 3–14.
3 (*a*) N. Koumura, Z.-S. Wang, S. Mori, M. Miyashita, E. Suzuki and K. Hara, *J. Am. Chem. Soc.*, 2006, **128**, 14256–14257; (*b*) S. Kim, J. Kwan Lee, S. O. Kang, J. Ko, J.-H. Yum, S. Fantacci, F. D. Angelis, D. D. Censo, M. K. Nazeeruddin and M. Grätzel, *J. Am. Chem. Soc.*, 2006, **128**, 16701–16707; (*c*) H. Choi, C. Baik, S. O. Kang, J. Ko, M.-S. Kang, M. K. Nazeeruddin and M. Grätzel, *Angew. Chem., Int. Ed.*, 2008, **47**, 327–330.
4 Y. Wu and W. Zhu, *Chem. Soc. Rev.*, 2013, **42**, 2039.
5 (*a*) Y. Wu, M. Marszalek, S. M. Zakeeruddin, Q. Zhang, H. Tian, M. Grätzel and W. Zhu, *Energy Environ. Sci.*, 2012, **5**, 8261–8272; (*b*) K. Pei, Y. Wu, W. Wu, Q. Zhang, B. Chen, H. Tian and W. Zhu, *Chem. – Eur. J.*, 2012, **18**, 8190–8200.
6 (*a*) S. Haid, M. Marszalek, A. Mishra, M. Wielopolski, J. Teuscher, J.-E. Moser, R. Humphry-Baker, S. M. Zakeeruddin, M. Grätzel and P. Bäuerle, *Adv. Funct. Mater.*, 2012, **22**, 1291–1302; (*b*) S. Qu, C. Qin, A. Islam, Y. Wu, W. Zhu, J. Hua, H. Tian and L. Han, *Chem. Commun.*, 2012, **48**, 6972–6974.
7 (*a*) S. Chaurasia, C.-Y. Hsu, H.-H. Chou and J. T. Lin, *Org. Electron.*, 2014, **15**, 378–390; (*b*) W. Ying, X. Zhang, X. Li, W. Wu, F. Guo, J. Li, H. Ågren and J. Hua, *Tetrahedron*, 2014, **70**, 3901–3908; (*c*) Y. Hua, J. He, C. Zhang, C. Qin, L. Han, J. Zhao, T. Chen, W.-Y. Wong, W.-K. Wong and X. Zhu, *J. Mater. Chem. A*, 2015, **3**, 3103–3112.
8 N. Blouin, A. Michaud, D. Gendron, S. Wakim, E. Blair, R. Neagu-Plesu, M. Belletête, G. Durocher, Y. Tao and M. Leclerc, *J. Am. Chem. Soc.*, 2008, **130**, 732–742.
9 J. Ohshita, M. Nodono, T. Watanabe, Y. Ueno, A. Kunai, Y. Harima, K. Yamashita and M. Ishikawa, *J. Organomet. Chem.*, 1998, **553**, 487–491.
10 J. Ohshita, *Macromol. Chem. Phys.*, 2009, **210**, 1360–1370.
11 (*a*) T.-Y. Chu, J. Lu, S. Beaupré, Y. Zhang, J.-R. Poulio, S. Wakim, J. Zhou, M. Leclerc, Z. Li, J. Ding and Y. Tao, *J. Am. Chem. Soc.*, 2011, **133**, 4250–4253; (*b*) J. Ohshita, Y.-M. Hwang, T. Mizumo, H. Yoshida, Y. Ooyama, Y. Harima and Y. Kunugi, *Organometallics*, 2011, **30**, 3233–3236; (*c*) C. M. Amb, S. Chen, K. R. Graham, J. Subbiah, C. E. Small, F. So and J. R. Reynolds, *J. Am. Chem. Soc.*, 2011, **133**, 10062–10065; (*d*) Y.-M. Hwang, J. Ohshita, Y. Harima, T. Mizumo, Y. Ooyama, Y. Morihara, T. Izawa, T. Sugioka and A. Fujita, *Polymer*, 2011, **52**, 3912–3916; (*e*) J. Ohshita, M. Miyazaki, D. Tanaka, Y. Morihara, Y. Fujita and Y. Kunugi, *Polym. Chem.*, 2013, **4**, 3116–3122; (*f*) J. Ohshita, M. Miyazaki, F.-B. Zhang, D. Tanaka and Y. Morihara, *Polym. J.*, 2013, **45**, 979–984; (*g*) D. Tanaka, J. Ohshita, Y. Ooyama and Y. Morihara, *Polym. J.*, 2013, **45**, 1153–1158; (*h*) F.-B. Zhang, J. Ohshita, M. Miyazaki, D. Tanaka and Y. Morihara, *Polym. J.*, 2014, **46**, 628–631; (*i*) J. Ohshita, M. Miyazaki, M. Nakashima, D. Tanaka, Y. Ooyama, T. Sasaki, Y. Kunugi and Y. Morihara, *RSC Adv.*, 2015, **5**, 12686–12691.
12 (*a*) A. Kunai, J. Ohshita, T. Iida, K. Kanehara, A. Adachi and K. Okita, *Synth. Met.*, 2003, **137**, 1007–1008; (*b*) T. Lee, I. Jung, K. H. Song, H. Lee, J. Choi, K. Lee, B. J. Lee, J. Pak, C. Lee, S. O. Kang and J. Ko, *Organometallics*, 2004, **23**, 5280–5285; (*c*) K.-H. Lee, J. Ohshita, K. Kimura, Y. Kunugi and A. Kunai, *J. Organomet. Chem.*, 2005, **690**, 333–337; (*d*) J. Ohshita, D. Hamamoto, K. Kimura and A. Kunai, *J. Organomet. Chem.*, 2005, **690**, 3027–3032; (*e*) J. Ohshita, K. Kimura, K.-H. Lee, A. Kunai, Y.-W. Kwak, E.-C. Son and Y. Kunugi, *J. Polym. Sci., Part A: Polym. Chem.*, 2007, **45**, 4588–4596; (*f*) J. Ohshita, Y. Kurushima, K.-H. Lee, A. Kunai, Y. Ooyama and Y. Harima, *Organometallics*, 2007, **26**, 6591–6595; (*g*) J. Ohshita, M. Nakamura, K. Yamamoto, S. Watase and K. Matsukawa, *Dalton Trans.*, 2015, **44**, 8214–8220.
13 (*a*) W. Zeng, Y. Cao, Y. Bai, Y. Wang, Y. Shi, M. Zhang, F. Wang, C. Pan and P. Wang, *Chem. Mater.*, 2010, **22**, 1915–1925; (*b*) S. Ko, H. Choi, M.-S. Kang, H. Hwang, H. Ji, J. Kim, J. Ko and Y. Kang, *J. Mater. Chem.*, 2010, **20**, 2391–2399; (*c*) L.-Y. Lin, C.-H. Tsai, K.-T. Wong, T.-W. Huang, L. Hsieh, S.-H. Liu, H.-W. Lin, C.-C. Wu, S.-H. Chou, S.-H. Chen and A.-I. Tsai, *J. Org. Chem.*, 2010, **75**, 4778–4785; (*d*) F. M. Jradi, X. Kang, D. O'Neil, G. Pajares, Y. A. Getmanenko, P. Szymanski, T. C. Parker, M. A. El-Sayed and S. R. Marder, *Chem. Mater.*, 2015, **27**, 2480–2487; (*e*) F. M. Jradi, D. O'Neil, X. Kang, J. Wong, P. Szymanski, T. C. Parker, H. L. Anderson, M. A. El-Sayed and S. R. Marder, *Chem. Mater.*, 2015, **27**, 6305–6313.
14 G. C. Welch, R. C. Bakus II, S. J. Teat and G. C. Bazan, *J. Am. Chem. Soc.*, 2013, **135**, 2298–2305.

15 *Handbook of Chemistry and Physics*, ed. D. R. Lide, CRC Press, 76th edn, 1995–1996.
16 Y. Sun, S.-C. Chien, H.-L. Yip, Y. Zhang, K.-S. Chen, D. F. Zeigler, F.-C. Chen, B. Lin and A. K.-Y. Jen, *J. Mater. Chem.*, 2011, **21**, 13247–13255.
17 A. Hagfeldt, G. Boschloo, L. Sun, L. Kloo and H. Pettersson, *Chem. Rev.*, 2010, **110**, 6595–6663.
18 Y. Ooyama, S. Inoue, T. Nagano, K. Kushimoto, J. Ohshita, I. Imae, K. Komaguchi and Y. Harima, *Angew. Chem., Int. Ed.*, 2011, **50**, 7429–7433.